

DESY 97-099  
DAMTP-97-59  
June 1997

ISSN 0418-9833

# High- $p_{\perp}$ Jets in Diffractive Electroproduction

W. Buchmüller, M. F. McDermott

*Deutsches Elektronen-Synchrotron DESY, 22603 Hamburg, Germany*

and

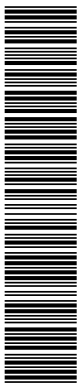
A. Hebecker

*D.A.M.T.P., Cambridge University, Cambridge CB3 9EW, England*

## Abstract

The diffractive production of high- $p_{\perp}$  jets in deep-inelastic scattering is studied in the semiclassical approach. The  $p_{\perp}$ -spectra of  $q\bar{q}$  and  $q\bar{q}g$  diffractive final states are found to be qualitatively different. For  $q\bar{q}$  final states, which are produced by 'hard' colour-singlet exchange, the  $p_{\perp}$ -spectrum is much softer than for  $q\bar{q}g$  final states, where the colour neutralization is 'soft'. Furthermore, the two different final states can be clearly distinguished by their diffractive mass distributions.

hep-ph/9706354 13 Jun 1997



The observation of high- $p_{\perp}$  jets in diffractive electron-proton scattering at small  $x$  [1] provides direct evidence for an intriguing interplay of ‘soft’ and ‘hard’ interactions in QCD. To disentangle these two aspects of diffractive deep-inelastic scattering detailed studies of different final states will be important.

One might expect the hard scale, provided by the transverse momentum of the jets, to ensure the applicability of perturbation theory. Indeed, the production of final states containing only two high- $p_{\perp}$  jets can be described by perturbative two-gluon exchange [2]. This process has been studied in detail by several groups and higher-order corrections have already partially been considered [3].

In this paper we study the diffractive production of high- $p_{\perp}$  jets in the semiclassical approach [4, 5]. In the proton rest frame, one calculates the high energy scattering of partonic fluctuations of the virtual photon by the colour field of the proton. We shall consider the two simplest configurations,  $q\bar{q}$  and  $q\bar{q}g$ . In both cases diffractive processes are obtained by projecting onto the colour singlet configuration of the final state partons.

The production of high- $p_{\perp}$  jets is dominated by  $q\bar{q}g$  final states where the gluon has low transverse momentum and carries a small energy fraction of the photon [5]. Kinetically, the presence of such a ‘wee’ parton in the photon implies that the fluctuation develops a large transverse size by the time it reaches the proton. The corresponding hard process is boson-gluon fusion [6]. We also calculate the  $p_{\perp}$ -spectrum for the  $q\bar{q}$  final state. With a proper identification of the inclusive gluon density one obtains the same result as two-gluon exchange in leading order. The two different final states can be directly distinguished by measuring the invariant mass of the two high- $p_{\perp}$  jets.

Our analysis is similar to the case of diffractive charm considered in [7]. Note however that in the present paper the production of both  $q\bar{q}$  and  $q\bar{q}g$  final states is described exclusively within the semiclassical approach.

## Hard and soft colour neutralization

In the semiclassical approach inclusive and diffractive cross sections can be expressed at leading order in terms of a single non-perturbative quantity,  $\text{tr} W_{x_{\perp}}^{\mathcal{F}}(y_{\perp})$ , where

$$W_{x_{\perp}}^{\mathcal{F}}(y_{\perp}) = U^{\dagger}(x_{\perp} + y_{\perp})U(x_{\perp}) - 1 \quad (1)$$

is built from the non-Abelian eikonal factors  $U$  and  $U^{\dagger}$  of the quark and antiquark whose light-like paths penetrate the colour field of the proton at transverse positions  $x_{\perp}$  and  $x_{\perp} + y_{\perp}$ , respectively (cf. Fig. 1). The superscript  $\mathcal{F}$  is used because the quarks are in the fundamental representation of the gauge group. Since the colour field outside the proton vanishes  $W_{x_{\perp}}^{\mathcal{F}}(y_{\perp})$  is essentially a closed Wilson loop through a section of the proton which measures an average of the proton colour field.

In an expansion in the transverse distance between quark and antiquark one has

$$\int_{x_{\perp}} \text{tr} W_{x_{\perp}}^{\mathcal{F}}(y_{\perp}) = -\frac{1}{4}y_{\perp}^2 C_1 + \mathcal{O}(y_{\perp}^4). \quad (2)$$

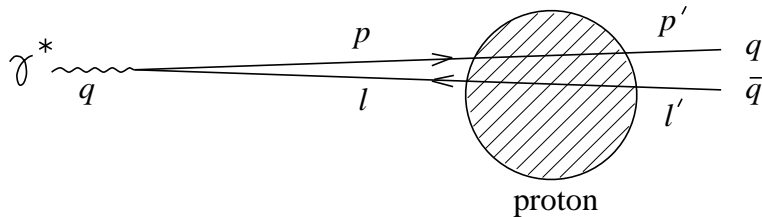


Figure 1: Exclusive two-jet production in the semiclassical approach.

Using the unitarity of the matrix  $U$  one can easily derive the constant

$$C_1 = \int_{x_\perp} \text{tr} \left( \partial_{y_\perp} W_{x_\perp}^{\mathcal{F}}(0) \partial_{y_\perp} W_{x_\perp}^{\mathcal{F}\dagger}(0) \right). \quad (3)$$

In the semiclassical approach this quantity determines the variation of the inclusive structure function  $F_2(x, Q^2)$  with  $Q^2$  [5]. A comparison with boson-gluon fusion in the parton model yields

$$C_1 = 2\pi^2 \alpha_s x G(x) \quad (4)$$

for the inclusive gluon density. Since  $C_1$  is constant  $G(x) \sim 1/x$  which corresponds to a classical bremsstrahl spectrum of gluons.

The integral over  $\text{tr} W_{x_\perp}^{\mathcal{F}}(y_\perp)$  in Eq. (2) describes the cross section,  $\sigma(y_\perp)$ , for the scattering of a colour dipole of transverse size  $y_\perp$  off the proton, within the semiclassical approach. A corresponding relationship between  $\sigma(y_\perp)$  and the inclusive gluon density is given in [8].

We now consider the production of a diffractive  $q\bar{q}$  final state. Using the results of [5] (cf. Appendix B) for the transversely polarized photon one easily finds

$$\left. \frac{d\sigma_T}{dt} \right|_{t=0} = \frac{\sum_q e_q^2 \alpha_{em}}{6(2\pi)^6} \int d\alpha dl_\perp^2 (\alpha^2 + (1-\alpha)^2) \left| \int_{x_\perp, y_\perp, l_\perp} e^{iy_\perp(l'_\perp - l_\perp)} \text{tr} W_{x_\perp}^{\mathcal{F}}(y_\perp) \frac{l_\perp}{a^2 + l_\perp^2} \right|^2, \quad (5)$$

$$a^2 = \alpha(1-\alpha)Q^2. \quad (6)$$

Here  $t = (q - p' - l')^2$  is the momentum transfer to the proton and  $\alpha = l'_0/q_0$ . The cross section for large transverse momenta is dominated by the short distance behaviour of  $\text{tr} W_{x_\perp}^{\mathcal{F}}(y_\perp)$ . Inserting Eq. (2), substituting  $y_\perp^2 \rightarrow -(\partial/\partial l_\perp)^2$  and using  $l'_\perp \simeq -p'_\perp$ , one obtains

$$\left. \frac{d\sigma_T}{dt d\alpha dp_\perp'^2} \right|_{t=0} = \frac{\sum_q e_q^2 \alpha_{em} C_1^2}{384\pi^2} (\alpha^2 + (1-\alpha)^2) \left| \left( \frac{\partial}{\partial p'_\perp} \right)^2 \frac{p'_\perp}{a^2 + p_\perp'^2} \right|^2. \quad (7)$$

As the derivation illustrates, this cross section describes the interaction of a small  $q\bar{q}$  pair with the proton. Hence, it is perturbative or hard. According to Eq. (4) the cross section Eq. (7) is proportional to the square of the gluon density. In order to obtain the integrated cross section one has to multiply Eq. (7) by the constant

$$C = \left( \int \frac{d\sigma}{dt} dt \right) / \left( \left. \frac{d\sigma}{dt} \right|_{t \approx 0} \right) \sim \Lambda^2, \quad (8)$$

where  $\Lambda$  is a typical hadronic scale. The resulting cross section integrated down to the transverse momentum  $p'_{\perp, \text{cut}}$  yields a contribution to the diffractive structure function  $F_2^D$  which is suppressed by  $\Lambda^2/p'_{\perp, \text{cut}}$ .

As shown in [5], a ‘leading twist’ cross section with jets of  $p_{\perp} \sim Q$  requires at least three partons in the final state, one of which has low transverse momentum. The corresponding cross sections can be written as convolution of ordinary partonic cross sections with diffractive parton densities [9]. In the case of high- $p_{\perp}$  quark jets there is an additional wee gluon (cf. Fig. 2). The partonic process is then boson-gluon fusion and the cross section

$$\frac{d\sigma_T}{d\xi dp'_{\perp}} = \int_x^{\xi} dy \frac{d\hat{\sigma}_T^{*g \rightarrow q\bar{q}}(y, p'_{\perp})}{dp'_{\perp}} \frac{dg(y, \xi)}{d\xi} \quad (9)$$

involves a diffractive gluon density [6]

$$\frac{dg(y, \xi)}{d\xi} = \frac{1}{8\xi^2} \left( \frac{b}{1-b} \right) \int \frac{d^2 k'_{\perp} (k'^2_{\perp})^2}{(2\pi)^4} \int_{x_{\perp}} \left| \int \frac{d^2 k_{\perp} \text{tr}[\tilde{W}_{x_{\perp}}^{\mathcal{A}}(k'_{\perp} - k_{\perp})] t^{ij}}{(2\pi)^2 k'_{\perp} b + k_{\perp}^2 (1-b)} \right|^2, \quad (10)$$

$$t^{ij} = \delta^{ij} + \frac{2k_{\perp}^i k_{\perp}^j}{k'_{\perp}{}^2} \left( \frac{1-b}{b} \right). \quad (11)$$

Here  $\xi = x(Q^2 + M^2)/Q^2$  for a final state with diffractive mass  $M$ , the momentum fraction of the proton carried by the incoming gluon is denoted by  $y$ , and  $b = y/\xi$ . The function  $\tilde{W}_{x_{\perp}}^{\mathcal{A}}$  is the Fourier transform of  $W_{x_{\perp}}^{\mathcal{A}}$  which is defined as in Eq. (1) but with the  $U$ -matrices in the adjoint representation, hence the superscript  $\mathcal{A}$ .

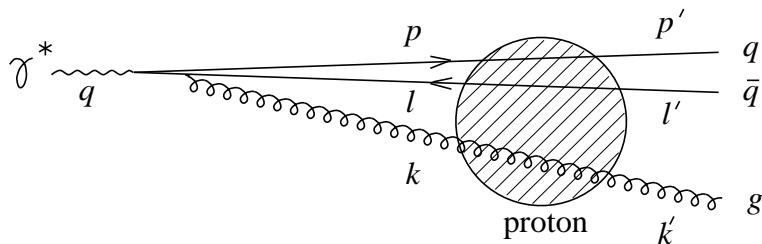


Figure 2: Two-jet production with an additional low transverse momentum gluon.

Eq. (9) is formulated in the partonic language which is appropriate in a frame in which the proton is fast. The corresponding process is shown in Fig. 3: a low transverse momentum colour-singlet pair of gluons is extracted from the proton, which is elastically scattered. One of the gluons, corresponding to the initial state off-shell gluon in Fig. 2, produces a high- $p_{\perp}$  pair of quark jets via boson-gluon fusion. Hence, the hard process is the same as in the diffractive parton model proposed in [10]. However, in contrast to this model, the semiclassical approach predicts an additional low transverse momentum gluon in the final state, which reflects the non-perturbative mechanism of colour neutralization.

In addition to boson-gluon fusion, the QCD Compton process can also produce high- $p_{\perp}$  jets. In this case either the quark or the antiquark is the wee parton. The corresponding

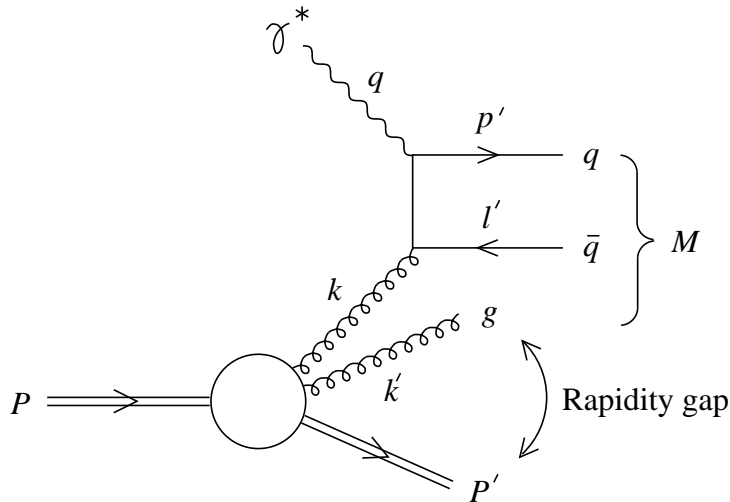


Figure 3: Interpretation of the process of Fig. 2 in terms of boson-gluon fusion in a frame where the proton is fast, e.g., the Breit frame.

cross section can be expressed in terms of a diffractive quark density [6],

$$\frac{d\sigma_T}{d\xi dp_{\perp}^{\prime 2}} = \int_x^{\xi} dy \frac{d\hat{\sigma}_T(y, p'_{\perp})^{\gamma^* q \rightarrow gq}}{dp_{\perp}^{\prime 2}} \frac{dq(y, \xi)}{d\xi}, \quad (12)$$

$$\frac{dq(y, \xi)}{d\xi} = \frac{2}{3\xi^2} \int \frac{d^2 l'_{\perp} (l_{\perp}^{\prime 2})}{(2\pi)^4} \int_{x_{\perp}} \left| \int \frac{d^2 l_{\perp}}{(2\pi)^2} \frac{l_{\perp} \text{tr}[\tilde{W}_{x_{\perp}}^{\mathcal{F}}(l'_{\perp} - l_{\perp})]}{l_{\perp}^2 b + l_{\perp}^2 (1-b)} \right|^2. \quad (13)$$

An analogous relation holds in the antiquark case.

The diffractive quark and gluon densities depend on  $\text{tr}\tilde{W}_{x_{\perp}}$  which is a function of the transverse momentum transfer to the wee parton. The integration is dominated by small values of this momentum transfer (of order  $\Lambda^2$ ). Hence, the diffractive quark and gluon densities are non-perturbative quantities which describe a soft interaction of the virtual photon with the proton.

We will not discuss the energy dependence of the above contributions to the diffractive jet cross section. For a given diffractive mass the energy dependence in the semi-classical approach is flat in both cases. However, this dependence will be increased by higher-loop corrections.

## Transverse momentum distribution of diffractive jets

The cross sections of Eqs. (9), (12) for diffractive boson-gluon fusion and diffractive Compton scattering, respectively, can be evaluated along the lines described in [7]. Therefore, in the following, we just list the relevant results. In the leading- $\ln(1/x)$  approximation one obtains for the longitudinal and transverse boson-gluon fusion cross

sections

$$\frac{d\sigma_L}{d\alpha dp_\perp'^2} = \frac{\Sigma_q e_q^2 \alpha_{em} \alpha_s}{2\pi^3} \frac{[\alpha(1-\alpha)]^2 Q^2 p_\perp'^2}{(a^2 + p_\perp'^2)^4} \ln(1/x) h_{\mathcal{A}}, \quad (14)$$

$$\frac{d\sigma_T}{d\alpha dp_\perp'^2} = \frac{\Sigma_q e_q^2 \alpha_{em} \alpha_s}{16\pi^3} \frac{(\alpha^2 + (1-\alpha)^2) (p_\perp'^4 + a^4)}{(a^2 + p_\perp'^2)^4} \ln(1/x) h_{\mathcal{A}}, \quad (15)$$

$$h_{\mathcal{A}} = \int_{y_\perp} \int_{x_\perp} \frac{|\text{tr} W_{x_\perp}^{\mathcal{A}}(y_\perp)|^2}{y_\perp^4}. \quad (16)$$

Similarly, one finds for the QCD-Compton cross sections

$$\frac{d\sigma_L}{d\alpha dp_\perp'^2} = \frac{16\Sigma_q e_q^2 \alpha_{em} \alpha_s}{27\pi^3} \frac{Q^2}{[\alpha(1-\alpha)] N^6} h_{\mathcal{F}}, \quad (17)$$

$$\frac{d\sigma_T}{d\alpha dp_\perp'^2} = \frac{4\Sigma_q e_q^2 \alpha_{em} \alpha_s}{27\pi^3 N^6 p_\perp'^2} \left[ N^4 - 2Q^2(N^2 + Q^2) + \frac{N^4 + Q^4}{\alpha(1-\alpha)} \right] h_{\mathcal{F}}, \quad (18)$$

$$N^2 = Q^2 + \frac{p_\perp'^2}{\alpha(1-\alpha)}, \quad (19)$$

where the constant  $h_{\mathcal{F}}$  is defined analogously to Eq. (16).

Comparing Eqs. (14), (15) with Eqs. (17), (18) we see that the configurations with a wee gluon are enhanced by  $\ln(1/x)$  at small  $x$  relative to those with a wee quark or antiquark. The simple arguments concerning colour outlined in [7] suggest an additional large suppression of the wee fermion contributions due to colour factors ( $h_{\mathcal{A}} \approx 16h_{\mathcal{F}}$ ). As a result we claim that the configurations with a wee gluon dominate over those with a wee fermion in the small- $x$  region relevant to diffraction and we shall ignore the latter from now on.

We can also calculate the differential cross section for the leading order  $q\bar{q}$  fluctuation, as described in the previous section (cf. Eq. (7)). The longitudinal and transverse cross sections are

$$\frac{d\sigma_L}{d\alpha dp_\perp'^2} = \frac{2\Sigma_q e_q^2 \alpha_{em} \alpha_s^2 \pi^2 [\xi G(\xi)]^2 C}{3} \frac{[\alpha(1-\alpha)]^2 Q^2 (a^2 - p_\perp'^2)^2}{(a^2 + p_\perp'^2)^6}, \quad (20)$$

$$\frac{d\sigma_T}{d\alpha dp_\perp'^2} = \frac{2\Sigma_q e_q^2 \alpha_{em} \alpha_s^2 \pi^2 [\xi G(\xi)]^2 C}{3} \frac{(\alpha^2 + (1-\alpha)^2) p_\perp'^2 a^4}{(a^2 + p_\perp'^2)^6}. \quad (21)$$

Identical differential distributions have been found for two-gluon exchange in leading order [3]. One can easily see that the region of  $\alpha$  close to zero or one dominates and that high- $p_\perp$  configurations are unlikely. We now attempt to quantify this statement.

The quantitative differences between the  $q\bar{q}$  and  $q\bar{q}g$  configurations are particularly pronounced in the integrated cross section with a lower cut on the transverse momentum of the quarks. Since the overall normalization of the contributions is uncertain (it is inherently non-perturbative) we compare the shape in  $p_\perp'^2$  of each configuration by

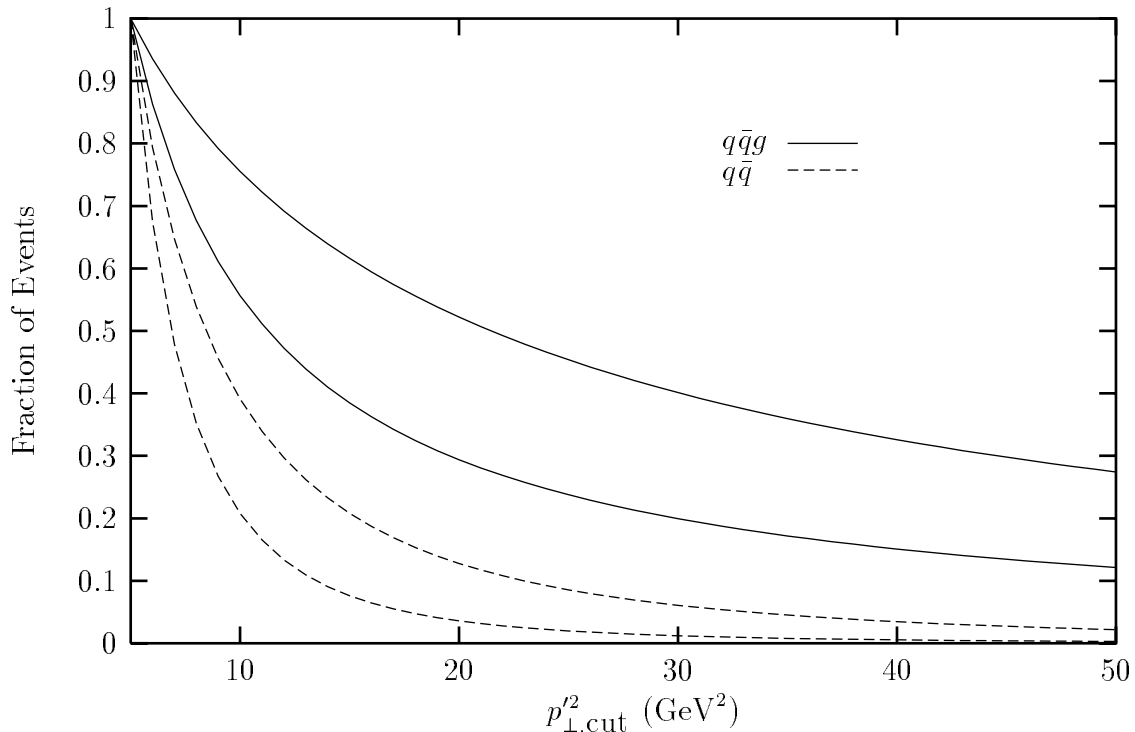


Figure 4: The fraction of diffractive events with  $p_{\perp}^2$  above  $p_{\perp,\text{cut}}^2$  for  $Q^2$  of 10  $\text{GeV}^2$  and 100  $\text{GeV}^2$  (lower and upper curve in each pair).

considering the quantity

$$\sigma(p_{\perp,\text{cut}}^2) = \int_{p_{\perp,\text{cut}}^2}^{\infty} dp_{\perp}^2 \int_0^1 d\alpha \frac{d\sigma}{dp_{\perp}^2 d\alpha} \quad (22)$$

which is the fraction of events remaining above a certain minimum  $p_{\perp}^2$ . The integrand here is obtained by adding the contributions from longitudinal and transverse photons, in each case. Fig. 4 shows the dependence of the corresponding event fraction on the lower limit,  $p_{\perp,\text{cut}}^2$ . Each curve is normalized to its value at  $p_{\perp,\text{cut}}^2 = 5 \text{ GeV}^2$ . One can see that the spectrum for the  $q\bar{q}g$  configuration is much harder than that for the  $q\bar{q}$  configuration. This is expected since in boson-gluon fusion  $p_{\perp}$  is distributed logarithmically between the soft scale and  $Q$  thus resulting in a significant high- $p_{\perp}$  tail above  $p'_{\perp,\text{cut}}$ .

## Mass distribution of the diffractive jet system

Let  $M_j$  be the invariant mass of the two-jet system in diffractive events containing two high- $p_{\perp}$  jets in the diffractive final state. The measurement of this observable provides, in principle, a clean distinction between  $q\bar{q}$  final states, where  $M_j^2 = M^2$ , and  $q\bar{q}g$  final states, where  $M_j^2 < M^2$ . In practice, however, this requires the contribution of the wee gluon to the diffractive mass, which is responsible for the difference between  $M^2$  and  $M_j^2$ , to be sufficiently large. To quantify the expectation within the semiclassical approach we

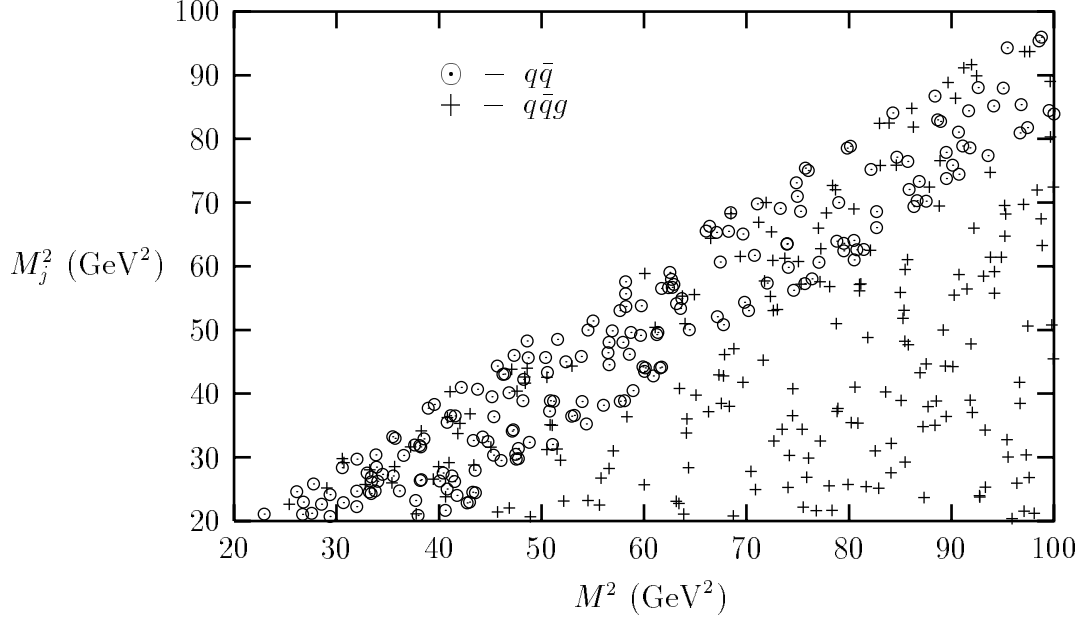


Figure 5: Distributions in  $M^2$  and  $M_j^2$  of diffractive events originating from  $q\bar{q}$  and  $q\bar{q}g$  final states for  $Q^2 = 50 \text{ GeV}^2$ ,  $p_{\perp,\text{cut}}^2 = 5 \text{ GeV}^2$  and  $C_g = 1$ .

consider the transverse photon contribution to the differential diffractive cross section  $d\sigma/dM^2 dM_j^2$ .

In the case of a  $q\bar{q}$  final state this cross section can be obtained directly from Eq. (21),

$$\frac{d\sigma_T}{dM^2 dM_j^2} = \Sigma_q e_q^2 \alpha_{em} \alpha_s^2 \pi^2 [\xi G(\xi)]^2 C \delta(M^2 - M_j^2) \frac{16M^2 Q^4 \sqrt{1-\kappa}}{3(M^2 + Q^2)^6 \kappa}. \quad (23)$$

Here the  $\delta$ -function setting  $M^2 = M_j^2$  is only precise up to hadronization effects, which are expected to be of the order of the hadronic scale. The dependence on the transverse momentum cutoff enters via the variable  $\kappa = 4p_{\perp,\text{cut}}^2/M_j^2$ .

In contrast, the mass distribution for diffractive processes with three-particle final states is not peaked at  $M_j^2 = M^2$ . Concentrating, as before, on the transverse photon polarization and on the contribution from the diffractive gluon density the following formula can be derived from Eq. (9)

$$\frac{d\sigma_T}{dM^2 dM_j^2} = 2\pi \Sigma_q e_q^2 \alpha_{em} \alpha_s y^2 \frac{dg(y, \xi)}{d\xi} \frac{Q^4 + M_j^4}{(Q^2 + M_j^2)^5} \left[ 2 \text{Arctanh} \sqrt{1-\kappa} - \sqrt{1-\kappa} \right]. \quad (24)$$

Simple algebra shows that  $y^2(dg(y, \xi)/d\xi)$ , formally a function of  $y$  and  $\xi$ , depends in fact only on the single variable  $u = \xi/y - 1$ ,

$$y^2 \frac{dg(y, \xi)}{d\xi} = \frac{1}{8u} \int \frac{d^2 k'_\perp}{(2\pi)^4} (k'_\perp{}^2)^2 \int_{x_\perp} \left| \int \frac{d^2 k_\perp}{(2\pi)^2} \left( \delta^{ij} + \frac{2k_\perp^i k_\perp^j}{k_\perp'^2} u \right) \frac{\text{tr} \tilde{W}_{x_\perp}^A(k'_\perp - k_\perp)}{k_\perp'^2 + u k_\perp^2} \right|^2. \quad (25)$$



As has been argued in [7], a simple parameterization of this function, consistent with the concept of a smooth localized colour field, is given by

$$y^2 \frac{dg(y, \xi)}{d\xi} \propto \frac{1}{C_g + u}, \quad (26)$$

where  $C_g$  is a constant of  $\mathcal{O}(1)$ . It has been checked that the precise value of the constant  $C_g$  does not affect the qualitative features of the mass distribution (compare the analysis of [7]).

To illustrate the experimental implications of Eqs. (23) and (24) we have shown in Fig. 5 the positions in  $M^2$  and  $M_j^2$  of two sets of 200 events, scattered randomly according to the distributions given above. The  $\delta$ -function of the  $q\bar{q}$  case has been replaced by a uniform distribution of  $M_j^2$  in a band  $M^2 > M_j^2 > M^2 - 20 \text{ GeV}^2$ . This allows for hadronization effects and, more importantly, for a large experimental uncertainty of the mass of the jet system. The scatter plot clearly exhibits the distinctive features of the two underlying partonic processes, even for this limited number of events. With sufficient statistics a determination of the relative weight of soft colour-singlet exchange, relevant in the  $q\bar{q}g$  case, and hard colour-singlet exchange, relevant in the  $q\bar{q}$  case, should be feasible.

## Conclusions

The  $p_\perp$ -spectrum and the diffractive mass distribution for two different diffractive final states,  $q\bar{q}$  and  $q\bar{q}g$ , have been evaluated in the semiclassical approach.

At high- $p_\perp$ , a  $q\bar{q}$  final state is produced by hard colour-singlet exchange. The corresponding  $p_\perp$ -spectrum is identical with the result of two-gluon exchange in leading order. In contrast, high- $p_\perp$  jets in  $q\bar{q}g$  final states are predominantly produced via boson-gluon fusion. The colour neutralization mechanism is soft and the cross section is proportional to a diffractive gluon density. This non-perturbative quantity describes the probability of extracting a colour-singlet pair of low transverse momentum gluons from the proton.

The  $q\bar{q}$  and  $q\bar{q}g$  final states also lead to qualitatively different diffractive mass distributions. Hence, like diffractive charm production, the study of diffractive high- $p_\perp$  jets should provide evidence for the relative importance of soft and hard contributions in diffractive deep-inelastic scattering.

## References

- [1] ZEUS collaboration, Phys. Lett. B332 (1994) 228;  
H1 collaboration, pa02-068, *Thrust Jet Analysis of Deep-Inelastic Large Rapidity Gap Events at HERA*, XXVIII ICHEP, Warsaw, 1996
- [2] A. H. Mueller, Nucl. Phys. B335 (1990) 115;  
M. G. Ryskin, Sov. J. Nucl. Phys. 52 (1990) 529;  
N. N. Nikolaev and B. G. Zakharov, Z. Phys. C53 (1992) 331

- [3] N.N. Nikolaev and B.G. Zakharov, J. Exp. Theor. Phys. 78 (1994) 598;  
M. Diehl, Z. Phys. C66 (1995) 181;  
J. Bartels, H. Lotter and M. Wüsthoff, Phys. Lett. B379 (1996) 239;  
J. Bartels and M. Wüsthoff, J. Phys. G22 (1996) 929;  
M. Wüsthoff, preprint ANL-HEP-PR-97-03, hep-ph/9702201
- [4] W. Buchmüller and A. Hebecker, Nucl. Phys. B476 (1996) 203
- [5] W. Buchmüller, M.F. McDermott and A. Hebecker, Nucl. Phys. B487 (1997) 283,  
erratum *ibid.*
- [6] A. Hebecker, preprint DAMTP-97-10, hep-ph/9702373
- [7] W. Buchmüller, M.F. McDermott and A. Hebecker,  
hep-ph/9703314, to appear in Phys. Lett. B
- [8] L. Frankfurt, G.A. Miller and M. Strikman, Phys. Lett. B304 (1993) 1
- [9] G. Ingelman and P.E. Schlein, Phys. Lett. B152 (1985) 256;  
L. Trentadue and G. Veneziano, Phys. Lett. B323 (1994) 201;  
A. Berera and D.E. Soper, Phys. Rev D50 (1994) 4328
- [10] W. Buchmüller and A. Hebecker, Phys. Lett. B355 (1995) 573